Galaxies point at each other and mess up measurements of the Universe. Now with rainbows*!

~~Redshift-dependent RSD bias from Intrinsic Alignment with DESI Year 1 Spectra~~

Claire Lamman,[1★] Daniel Eisenstein,[1] Jessica Nicole Aguilar,[2] Steven Ahlen,[3] David Brooks,[4] Todd Claybaugh,[2] Axel de la Macorra,[5] Arjun Dey,[6] Biprateep Dey,[7] Peter Doel,[4] Simone Ferraro,[2,8] Andreu Font-Ribera,[9] Jaime E. Forero-Romero,[11,12] Satya Gontcho A Gontcho,[2] Julien Guy,[2] Robert Kehoe,[13] Anthony Kremin,[2] Laurent L. Le Guillou,[14] Michael Levi,[2] Marc Manera,[9] Ramon Miquel,[9,15] Jeffrey A. Newman,[7] Jundan Nie,[16] Nathalie Palanque-Delabrouille,[17] Francisco Prada,[18] Mehdi Rezaie,[19] Graziano Rossi,[20] Eusebio Sanchez,[21] Michael Schubnell,[22] Seo Hee-Jong,[23] Gregory Tarlé,[22] Benjamin Alan Weaver,[6] Zhimin Zhou[24]

[1] Center for Astrophysics | Harvard & Smithsonian, 60 Garden Street, Cambridge, MA 02138, USA
[2] Lawrence Berkeley National Laboratory, 1 Cyclotron Road, Berkeley, CA 94720, USA
[3] Physics Dept., Boston University, 590 Commonwealth Avenue, Boston, MA 02215, USA
[4] Department of Physics & Astronomy, University College London, Gower Street, London, WC1E 6BT, UK
[5] Instituto de Física, Universidad Nacional Autónoma de México, Cd. de México C.P. 04510, México
[6] NSF's NOIRLab, 950 N. Cherry Ave., Tucson, AZ 85719, USA
[7] Department of Physics and Astronomy, University of Pittsburgh and Pittsburgh Particle Physics, Astrophysics, and Cosmology Center (PITT PACC), University of Pittsburgh, 3941 O'Hara Street, Pittsburgh, PA 15260, USA
[8] University of California, Berkeley, 110 Sproul Hall #5800 Berkeley, CA 94720, USA
[9] Institut de Física d'Altes Energies (IFAE), The Barcelona Institute of Science and Technology, Campus UAB, 08193 Bellaterra Barcelona, Spain
[10] Department of Physics & Astronomy, University College London, Gower Street, London, WC1E 6BT, UK
[11] Departamento de Física, Universidad de los Andes, Cra. 1 No. 18A-10, Edificio Ip, CP 111711, Bogotá, Colombia
[12] Observatorio Astronómico, Universidad de los Andes, Cra. 1 No. 18A-10, Edificio H, CP 111711 Bogotá, Colombia
[13] Department of Physics, Southern Methodist University, 3215 Daniel Avenue, Dallas, TX 75275, USA
[14] Sorbonne Université, CNRS/IN2P3, Laboratoire de Physique Nucléaire et de Hautes Energies (LPNHE), FR-75005 Paris, France
[15] Institució Catalana de Recerca i Estudis Avançats, Passeig de Lluís Companys, 23, 08010 Barcelona, Spain
[16] National Astronomical Observatories, Chinese Academy of Sciences, A20 Datun Rd., Chaoyang District, Beijing, 100012, P.R. China
[17] IRFU, CEA, Université Paris-Saclay, F-91191 Gif-sur-Yvette, France
[18] Instituto de Astrofísica de Andalucía (CSIC), Glorieta de la Astronomía, s/n, E-18008 Granada, Spain
[19] Department of Physics, Kansas State University, 116 Cardwell Hall, Manhattan, KS 66506, USA
[20] Department of Physics and Astronomy, Sejong University, Seoul, 143-747, Korea
[21] CIEMAT, Avenida Complutense 40, E-28040 Madrid, Spain
[22] University of Michigan, Ann Arbor, MI 48109, USA
[23] Department of Physics & Astronomy, Ohio University, Athens, OH 45701, USA
[24] National Astronomical Observatories, Chinese Academy of Sciences, A20 Datun Rd., Chaoyang District, Beijing, 100012, P.R. China

People all over the world collaborated to get the data we use in this paper

Accepted XXX. Received YYY; in original form ZZZ

INFORMATION-DENSE SUMMARY

ABSTRACT

We estimate the redshift-dependent, anisotropic clustering signal in DESI's Year 1 Survey created by tidal alignments of ...

There will be an unusual clustering pattern in DESI's map of galaxies. It's created by two effects: galaxy orientations are correlated with the underlying dark matter, and galaxy orientations are biased by the way we choose galaxies. Both effects are correlated with galaxy distance, which we can now measure with DESI's spectra. This clustering pattern is the same pattern we use to measure how fast the cosmic web grows, and the balance between dark energy and gravity! This is a problem but we can fix it with the results here.

★ E-mail: claire.lamman@cfa.harvard.edu

*by "rainbows" I mean spectra. More on this later...

BACKGROUND INFO

You may have heard that telescopes are time machines because light takes time to travel. Light from a star that's one light year away takes a year to get to Earth, so we see that star as it existed one year in the past.

Cosmologists take this idea to the extreme and look at how the Universe itself changes over millions of years.

We do this by mapping out the massive web of dark matter in the Universe, as traced by glowing galaxies. Over time, gravity draws stuff together and the web becomes more webby.

However, it's growing slightly slower than you'd expect from gravity alone... So what's up? Is gravity slacking? Is Einstein a liar?

Probably not.

There's a mysterious force out there acting against gravity:

Dark Energy

LPT: Telescopes are by far the safest way to travel in time

If aliens 10 light years away are detecting Earth TV signals, they are just about to watch the final season of Breaking Bad...

No S Po I L Er S

To figure out more, we need a very big map of galaxies...

This is where "DESI" comes in, the Dark Energy Spectroscopic Instrument. We're measuring the positions of 40 million galaxies and making the most complete map of the nearby Universe.

DESI will measure how fast the cosmic web grows, revealing the balance between gravity and dark energy. In this paper, we explore an effect that will bias these important measurements.

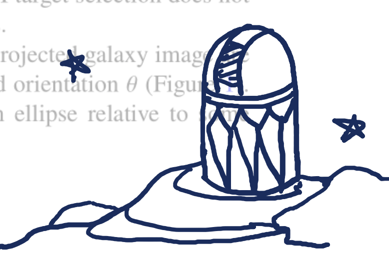

For a similar paper summary on Dark Energy, see this link
For a similar paper summary on a related paper, see this link.

This is what a galaxy looks like to a cosmologist (apologies to other astronomers)

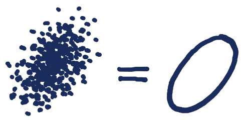

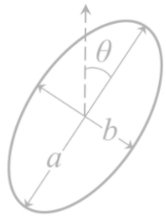

Figure 1. The parameters used to describe the shape and orientation of the ellipse created by projecting an elliptical galaxy. Here, the ellipticity is measured relative to North. For our measurement, ellipticity is measured relative to the position of the tracer sample.

GALAXY PICTURES

direction using ϵ_+:

$$\epsilon_+ = \frac{a-b}{a+b}\cos(2\theta) \tag{1}$$

We have lovely pictures of each galaxy, which is how we get information about their shape.

DESI's LRG target selection from this catalog includes a cut based on the [illegible] flux [illegible] within a DESI fiber, which corresponds to a 1.5 arcsec diameter aperture. The z-band magnitude within the aperture is limited to z_{fiber} < 21.61 in the Northern Galactic Cap and $z_{\text{fiber}} < 21.60$ in the Southern Galactic Cap. For more information DESI's target selection, see Raichoor et al. (2020); Zhou et al. (2020, 2022).

To us, every galaxy is an oval and this is the math we use to describe its shape and orientation.

This shape fitting and target selection is dependent upon imaging quality, which varies across sky regions. To quantify the effect of imaging [illegible] the LRGs into three sky regions: The MzLS and BASS region, the DECaLS region which does not contain DES imaging, and the DES region. We compare the reported axis ratio, b/a, of the reported galaxy shapes in each region in Figure 2. The MzLS and BASS region reports more eccentric LRG shapes than the other regions, and the region with highest-quality imaging, DES, reports the roundest shapes. While this may indicate an over-correcting of the PSF in MzLS and BASS imaging, we measure the IA signal independently in these regions and do not find any significant impact on final results (Section 3.2).

GALAXY RAINBOWS

2.2 Spectroscopy

The Universe is expanding. As distant galaxies move away from us, their light becomes stretched and reddened. Generally:

Redder = farther away

But it's a little more complicated than that. DESI can gather the light of each galaxy and split it up into a "rainbow", or spectrum.

Rainbows are important because each galaxy has a "spectral fingerprint" we can use to measure exactly how much the light is shifted and how far away the galaxy is.

We used spectra from DESI's internal data release, Iron, which is composed of data from commissioning through Year 1 of the survey (DESI Collaboration, in prep). It contains spectra of 2.9 million LRGs and 4.0 million ELGs from observations taken during December 14th, 2020 through June 13th 2022 (Zhou et al. 2022; Raichoor et al. 2023; Guy et al. 2023). We used Iron's large-scale structure catalog which includes a veto on targets based on hardware and imaging conditions. The catalog contains weights to account for completeness based on the probability that each target was assigned. LRGs also have a weight to account for redshift failures. From this catalog, we ran a basic redshift-quality cut to obtain our final samples of 2.5 million LRGs and 3.1 million ELGs.

The projected correlation functions used to calibrate our measurements (Section 3.2) [illegible]. Due to internal blinding policies, our estimation of DESI's ξ_2 measurements are calibrated with the smaller, publicly available spectroscopic catalog from DESI's Survey Validation (DESI Collaboration et al. 2023a,b; Lan et al. 2023). Our determination of the ξ_2 signal which arises from IA is independent of the RSD ξ_2 signal.

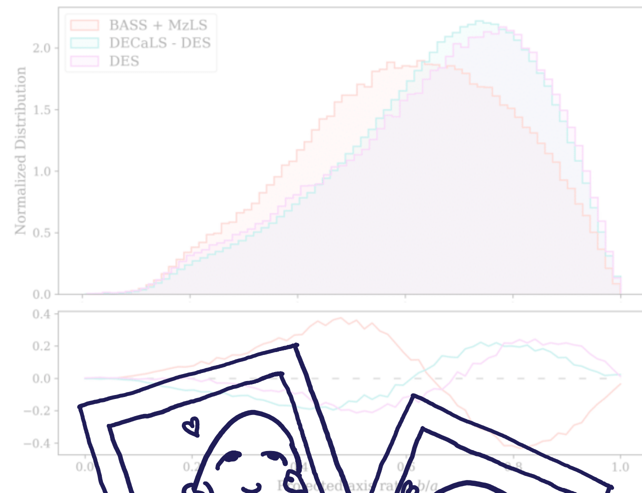

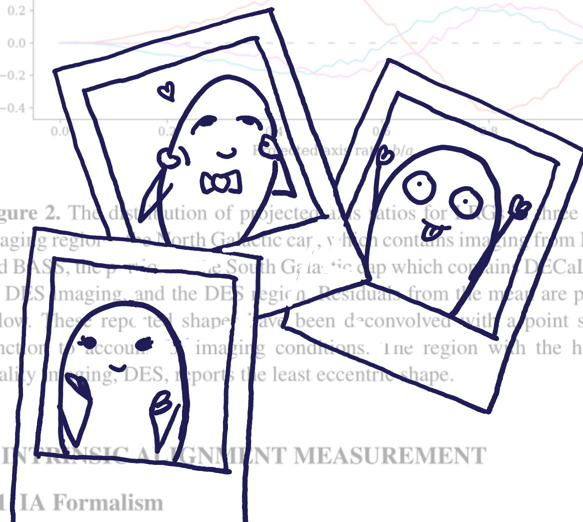

Figure 2. The distribution of projected axis ratios for LRGs in three DESI imaging regions: the North Galactic cap, which contains imaging from MzLS and BASS, the portion of the South Galactic cap which contains DECaLS but no DES imaging, and the DES region. Residuals from the mean are plotted below. These reported shapes have been deconvolved with a point spread function to account for imaging conditions. The region with the highest quality imaging, DES, reports the least eccentric shape.

3 INTRINSIC ALIGNMENT MEASUREMENT

3.1 IA Formalism

As in Lamman et al. (2023b), we measure the correlation between galaxy shapes and density by averaging the ellipticity of each LRG relative to the separation vector between it and nearby galaxies in the tracer sample[1].

$$\mathcal{E}(r_p) = \langle \epsilon_+(a, b, \theta) \rangle \tag{2}$$

For a given galaxy-tracer pair, a and b are the axis lengths of the galaxy shape and θ is the orientation of the galaxy relative to the separation vector between it and the tracer. This is measured as a function of the projected separation between them, r_p.

We limit the separation of pairs along the LOS, r_Π, to $\pm\Pi_{\text{max}} = 30h^{-1}$Mpc. This, along with clustering, is taken into account in our model when estimating how far along the LOS the IA measurement is averaged over.

For measuring the IA of our full LRG sample, we divide the tracer catalog into 100 sky regions based on right ascension and declination with an equal number of galaxies in each. $\mathcal{E}(r_p)$ is measured independently in each region using its tracers and the full shape catalog, then averaged over every pair. This average included the catalog weights described in Section 2.2 for both the shape and tracer samples. The average of these 100 measurements and standard error is our final measurement.

IA is often quantified using a form of correlation functions generalized to include information about galaxy shapes (Mandelbaum et al. 2006). The IA correlation function relating galaxy shapes and density is

$$\xi_{g+}(r_p) = \frac{S_+D - S_+R_D}{R_SR_D} \tag{3}$$

S_+D is the count of data-data pairs weighted by the orientation

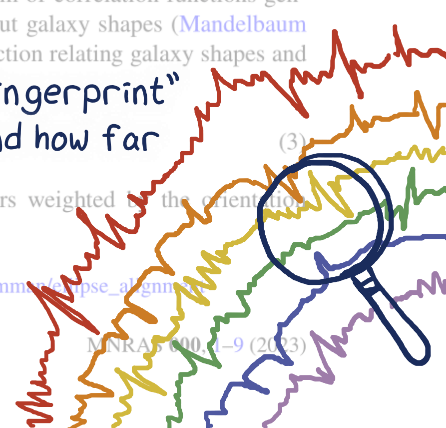

[1] code available here: github.com/cmlamman/ellipse_alignment

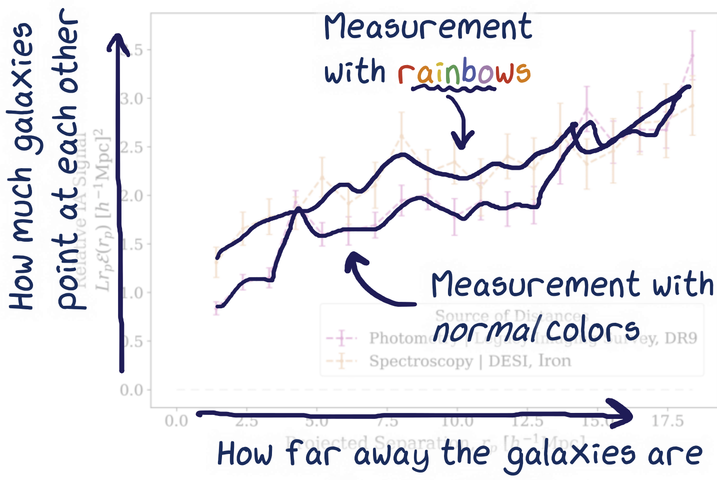

Figure 3. The IA signal of LRGs ... 0.4 < z < 1.1, compared to the estimate made in (Lamman et al. 2023b) with photometric distances. The photometric estimate was made with 17.5 million galaxies, compared to 2.5 million LRGs for the spectroscopic sample, but necessarily averaged over a larger radial distance. This is adjusted for here, which shows the "relative" IA signal that has been calibrated by the effective radial depth L.

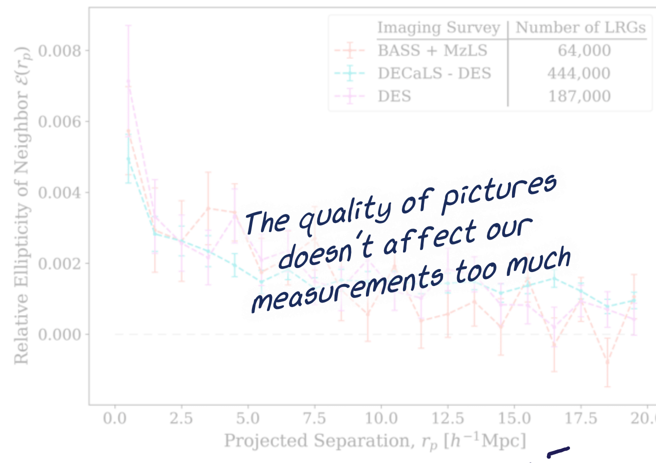

Figure 4. Measurement of the tidal alignment of LRG shapes made independently in areas from three regions of DESI's Legacy Imaging Survey described in Section 2.2. DES has the highest quality imaging, but there is no significant ... IA signal.

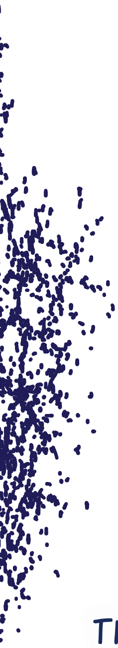

GALAXY SHAPES CONNECTED TO WEB

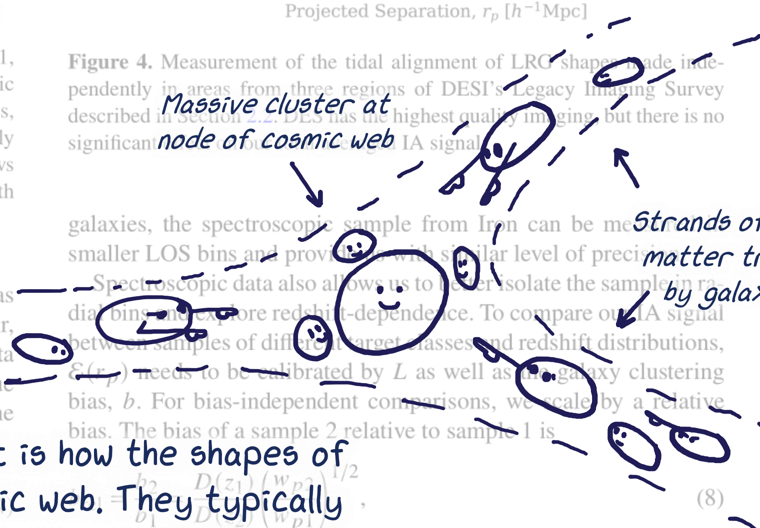

... er sample D. Measuring this as function of projected separation and averaging over each data pair, $S_+D(r_p)/DD(r_p)$, is equivalent to $\mathcal{E}(r_p)$. S_+R represents the data shapes relative to a random sample, which has an expectation value of 0. R_SR_D is the random-random count. Integrating ξ_{g+} along the LOS direction, Π, produces the projected IA correlation function:

The first part of our measurement is how the shapes of galaxies are connected to the cosmic web. They typically point towards other galaxies and dense areas, aligning along large strands of dark matter.

$$w_{g+}(r_p) = \int_{-\Pi_{max}}^{\Pi_{max}} ...$$

For predicting the RSD bias that arises from IA, $\mathcal{E}(r_p)$ is the most direct ... pairs, not randoms. DD can be expressed as

$$DD(r_p) = RR \int_{-\Pi_{max}}^{\Pi_{max}} d\Pi \frac{DD(r_p,\Pi)}{RR} = RR \int_{-\Pi_{max}}^{\Pi_{max}} d\Pi (1 + \xi(r_p,\Pi)) = RR(2\Pi_{max} + w_p(r_p)). \quad (5)$$

Here ξ and w_p are the typical correlation function and projected correlation function, as opposed to those weighted by shape alignments. w_{g+} can be expressed as

The math we use to describe how these shapes are connected to the cosmic web.

$$w_{g+}(r_p) = \frac{1}{RR}\int_{-\Pi_{max}}^{\Pi_{max}} d\Pi S_+D(r_p,\Pi) = \frac{S_+D(r_p)}{RR}. \quad (6)$$

Therefore, a given w_{g+} and $\mathcal{E}$ made with the same Π_{max} and same binning ... are related as

We take care to describe other ways people measure this and how they're related to our method.

$$w_{g+}(r_p) = (2\Pi_{max} + w_p(r_p))\mathcal{E}(r_p) = L\mathcal{E}(r_p) \quad (7)$$

Here we have introduced L, which can be understood as the effective LOS distance that $\mathcal{E}$ is measured ... adjusted to account for clustering which decreases the average LOS-separation of pairs. L is included in our final model of the RSD bias (Section 5)[2]. While $L\mathcal{E}$ is functionally equivalent to w_{g+}, we notate L and $\mathcal{E}$ separately to be explicit about how the quantity was estimated.

We can compare our spectroscopic IA measurement with a similar one made with photometric data (Lamman et al. 2023b) by scaling by L, as shown in Figure 3. Although made with several ...

[2] L here is equivalent to L_{eff} in Lamman et al. (2023b)

Galaxy NGC 5614: "complicated"

galaxies, the spectroscopic sample from Iron can be me... smaller LOS bins and provide ... with similar level of precision. Spectroscopic data also allows us to better isolate the sample in radial bins and explore redshift-dependence. To compare our IA signal between samples of different target classes and redshift distributions, $\mathcal{E}(r_p)$ needs to be calibrated by L as well as the galaxy clustering bias, b. For bias-independent comparisons, we scale by a relative bias. The bias of a sample 2 relative to sample 1 is

$$b_{rel} = \frac{b_2}{b_1} = \frac{D(z_1)}{D(z_2)}\left(\frac{w_{p2}}{w_{p1}}\right)^{1/2}, \quad (8)$$

where $D(z)$ is the linear growth function.

Therefore, when comparing IA measurements across samples we use the value $(L/b_{rel})\mathcal{E}(r_p)$. While L is taken into account when estimating the final RSD bias, b does not affect the final result. This is because the amplitude of the power spectrum quadrupole effect arises from the correlation of the galaxy density field and the selection-induced shape polarization, the latter of which is independent of bias.

When calculating distances and the growth factor, we assume a flat ΛCDM cosmology with $\Omega_m = 0.286$, $\Omega_\Lambda = 0.714$ and $H_0 = 69.6$ km s^{-1}Mpc^{-1}.

DO BAD PICTURES = BAD MEASUREMENTS?

2.3 Dependence on Imaging Region

The amplitude of IA can strongly depend upon imaging quality and the methods used to estimate shapes. This is in part due to difficulties in accurately modeling imaging processes, and in part due to isophotal twisting (Kasano & ... 199?) which causes the outer regions o... inner regions. This has been measured in BOSS LOWZ, DES, and LSST (Singh et al. 2015; Zuntz et al. 2018; Leonard et al. 2018; Georgiou et al. 201... ... imaging catalog, as imaging quality and shapes vary across region (Figure 4). A lower signal due to poor imaging will result in an underestimation ... RSD bias.

Unfortunately, real galaxies are more complicated than just ovals.

In this section we check that the way we measure galaxy shapes won't affect our results.

To qualify the impact of imaging quality, we compare our IA signal across the three different imaging regions used in the Legacy Imaging Survey: DES, DECaLS, and MzLS+BASS. Each region has varying survey completeness, so to avoid edge effects we made these

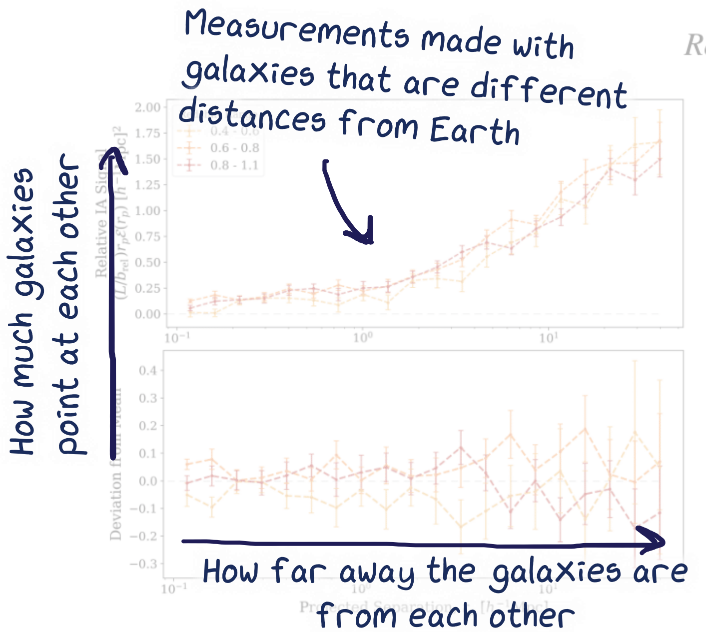

Figure 5. Comparison of the intrinsic alignment of LRGs between spectroscopic redshift bins. The y-axis is scaled by the effective depth of the measurement L and the galaxy bias $b_{\rm rel}$, which here is defined as $b_{\rm rel}(z = 0.7) = 1$. These were calculated using the projected correlation function from DESI's Year one data. Errors here only include the statistical difference of the signal between sky regions and not from b or L. Nearby galaxies broadly display a weaker alignment, though here we have not accounted for luminosity differences across samples.

measurements in a limited area with the most completeness in each region. The result and size of each sample is shown in Figure 4. We do not find a significant difference in the signals, which is in part due to [illegible] although the BASS +MzLS region may be over-correcting for the PSF and producing more [illegible] systematic imaging effects are uncorrelated with the tidal field. A small change in ellipticity doesn't propagate as an order-unity error on this signal, which is a very small response to the tidal shear. This may be still be an issue for higher signal-to-noise detections beyond DESI Year 1.

HOW THE MEASUREMENT CHANGES WITH DIFFERENT GALAXY SAMPLES

We split our galaxies into three samples based on how far away they are from Earth.

A [illegible] nent using the cross-component of shape, $\epsilon_\times = \frac{a-b}{a+b}\sin(2\theta)$ instead of [illegible] in Equation 2. This was consistent with 0 on all scales.

3.3 Dependence on Redshift and Tracer Sample

We see a slight difference in the signal between these samples, which we'll include in our final results.

The redshift dependence of IA is unclear (Samuroff et al. 2021; Zhou et al. [illegible]) [illegible] ot be directly observed without accounting for luminosity differences across redshift bins. DESI's LRG sample is designed to have a constant co-moving volume with [illegible] more luminous, and therefore more aligned, galaxies in high redshift samples. However, since we are only inferring a systematic bias and not any physical trends, we only require the IA of each sample. The IA RSD bias is proportional to the amplitude of this signal, so if not properly accounted for, it could manifest in DESI's results as a false evolution of the growth rate as measured by the quadrupole of the correlation function. Therefore we separate our LRG tracer sample into three sub-samples based on redshift and measure the correlation of LRG shapes in each.

The samples are plotted in Figure 5 and displayed in Table 1. To compare the strength of tidal alignment between redshifts, the signal is adjusted based on the clustering in each sample, as described in Section 3.1. As expected, we find the weakest signal for nearby galaxies (0.4 < z < 0.6).

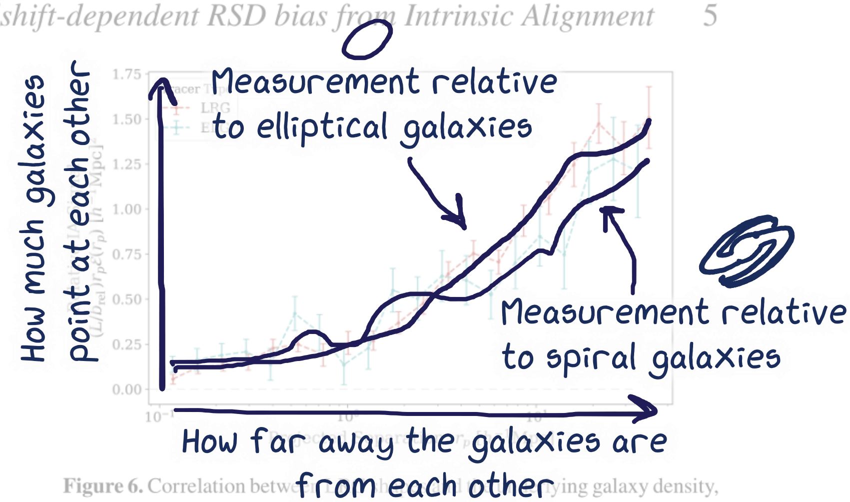

Figure 6. Correlation betw[illegible] [illegible]ying galaxy density, as traced by both LRGs and ELGs. These samples are both in the redshift range $0.8 < z < 1.1$. For comparison, this IA signal is scaled by the samples' clustering, as described in 3.1.

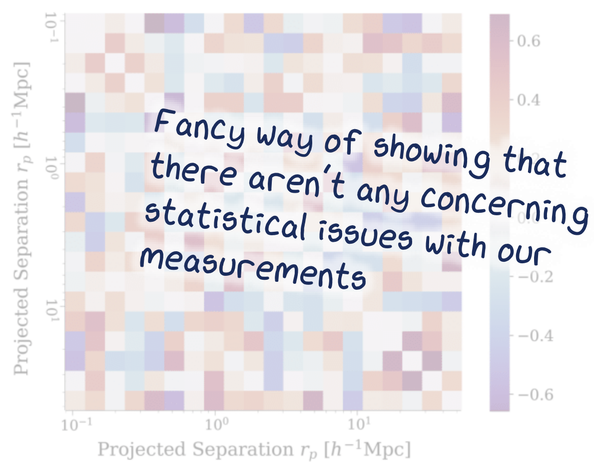

Figure 7. The reduced covariance matrix of $\mathcal{E}$ between bins of transverse separation for our IA measurement with LRG tracers across the full redshift range. The identity ma[illegible] subtracted from this plot. This demonstrates that there is n[illegible] evidence [illegible] correlations between the measurements of $\mathcal{E}$ in e[illegible] separation.

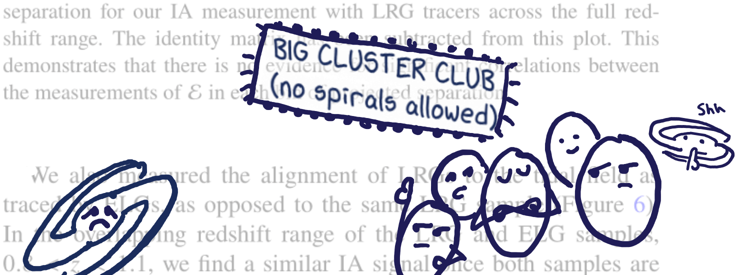

We also measured the alignment of LRGs to the tidal field as traced by ELGs, as opposed to the sam[illegible] (Figure 6). In the overlapping redshift range of the LRG and ELG samples, 0.[illegible] < z < 1.1, we find a similar IA signal since both samples are adjusted for clustering. Although some regions of DESI's Year one footprint are less complete for ELGs, this is accounted for in the catalog completeness weights described in Section 2 and we find no im[illegible] IA measurement.

Different types of galaxies trace the cosmic web in different ways. For example, big elliptical galaxies are more likely to be found in very dense areas over spiral galaxies.

A covariance matrix for the spectroscopic LRG measurement made over all redshift ranges is shown in Figure 7 and demonstrates no co[illegible] the bins of projected separation that the IA measurement $\mathcal{E}$ was made in.

4 SELECTION-INDUCED SHAPE POLARIZATION

Here we see how our results change if we measure galaxy shapes relative to the positions of spiral galaxies.

Th[illegible] galaxies are aligned along the tidal field (IA) and the degree to which ga[illegible] shape po[illegible] role in the redshift

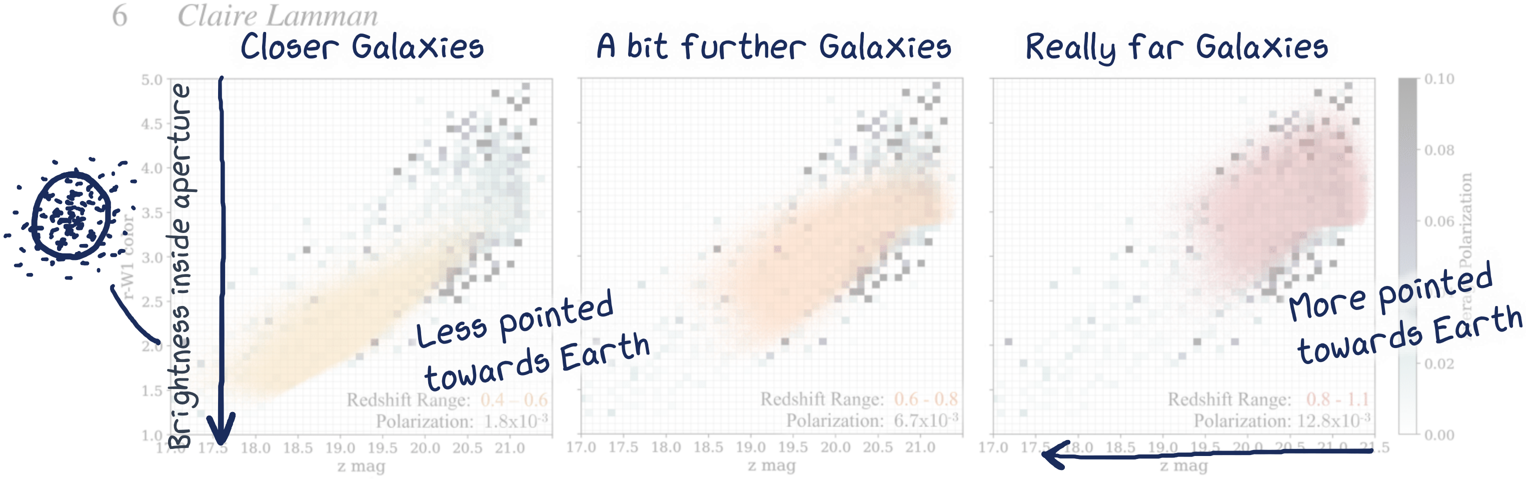

Figure 8. Estimates of shape polarization for each of the three redshift bins, or the tendency for these samples to have shapes aligned with the LOS due to an aperture magnitude cut. These are based on the model in (Lamman et al. 2023b), shown in grey, which estimates the polarization in bins of color and magnitude for a sample of LRGs [illegible]. The total polarization estimate for each redshift bin is the average of each galaxy's polarization corresponding to its respective color bin. The highest redshift sample contains redder, fainter galaxies which are closer to the survey cuts and therefore more likely to have biased galaxy orientations.

The redder, more distant galaxies are more affected by the bias in shape orientations.

GALAXIES ARE POINTING AT EARTH???

dependence of the RSD bias. Redder, fainter galaxies fall closer to the [illegible] cut that is used to select DESI targets. Therefore their orientation will have a stronger impact on whether or not they are selected; an elongated galaxy aligned with the LOS will have more light concentrated within a sky aperture.

Lamman et al. (2023b) estimated the shape polarization of DESI LRGs from a parent sample without the aperture-magnitude cut. This was done by generating many 3D light profiles for each galaxy based on the expe[illegible]es from Padilla & Strauss (2008). These light profiles were assigned random orientations then put through an aperture-magnitude cut. The average ellipticity of the selected sh[illegible] LOS [illegible] selection-induced shape polarization.

...well, not because we're special or anything. There's a VERY small tendency for galaxies to be pointing at us. And it's only in the sample of galaxies that DESI has chosen to observe.

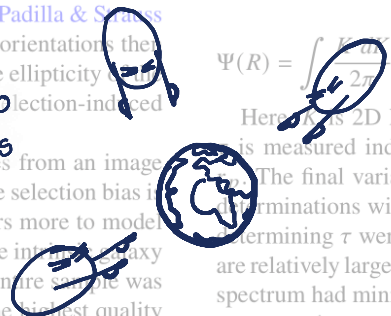

As this selection is done on aperture magnitudes from an image deconvolve[illegible] the shape selection bias is relatively independent of imaging quality. It matters more to model this effect with imaging that most closely reflects the intrinsic galaxy shape. The[illegible] for the entire sample was made using the portion of DESI's footprint with the highest quality imaging, the DES region. Although this results in a noisier measurement, only the average polarization of a sample affects the final RSD bias.

You can read more about why this is in a previous paper.

To estimate the polarization of the LRG redshift samples, we averaged the polarization estimates from the parent sample in bins of color and [illegible] polarization based on the average in their corresponding bin, and their total average is the polarization estimate of that sample. This was not done for the ELG sample, which were only used as tracers. A demonstration of this mapping can be see in Figure 8 and the results are also displayed in Table 1. It is important to note that the polarization varies more across redshift bins than the IA signal, meaning that the redshift dependence of the final RSD bias is more dependent on survey selection than physical alignments.

We took the results of that paper and looked at how this effect changes in samples of galaxies that are different distances away from Earth.

HOW IT ALL COMES TOGETHER

5 FALSE RSD SIGNATURE IN DESI

To estimate the RSD bias created by the combination of IA and the selection-induced polarization, we use a nonlinear tidal model adopted from La[illegible]

This next section connects everything talked about so far with the main thing we care about for this paper: How are the measurements of structure growth affected?

in this paper; we give only the results here. We have made minor notation changes for clarity.

The IA signal $\mathcal{E}$ is combined with the effective LOS-distance L, described in Section 3.1, and the nonlinear power spectrum P as τ:

$$\tau = \frac{2L(r_p)\mathcal{E}(r_p)}{r_p \frac{d}{dr_p}\left[\frac{1}{r_p}\Psi\right]}, \tag{9}$$

$$\Psi(R) = \int \frac{K\,dK}{2\pi}\frac{P(K)}{K}J_1(KR) \tag{10}$$

Here K is 2D Fourier Space and J_1 is the first Bessel function. [illegible] is measured independently in each bin of transverse separation, [illegible]. The final variable used in our result, $\bar{\tau}$, is the average of these determinations with standard error. The transverse bins we used for determining τ were linear bins between $5 - 20h^{-1}$Mpc. Since these are relatively large scales, the change from a linear to nonlinear power spectrum had minimal effects on our final result, though it produced more consistent values of τ across the transverse bins.

The "false" signature this produces in the quadrupole of the correlation function, $\xi_{2,\,\mathrm{gI}}$, is

$$\xi_{2,\,\mathrm{gI}}(s) = \epsilon_{\mathrm{LOS}}\frac{\bar{\tau}}{2\sigma^2_{E1}}\int\frac{q^2dq}{2\pi^2}P(q)j_2(qs). \tag{11}$$

Here, ϵ_{LOS} is the selection-induced shape polarization, σ^2_{E1} is the variance of the shape parameter ϵ_+ described in Section 2, j_2 is the second spherical Bessel function, and s is 3D separation. The relations most relevant for this study can be summarized as

$$\xi_{2,\,\mathrm{gI}} \propto \epsilon_{\mathrm{LRG}}\frac{\bar{\tau}}{\sigma^2_{E1}} \propto \epsilon_{\mathrm{LRG}}\frac{L\mathcal{E}}{\sigma^2_{E1}}. \tag{12}$$

Note that this result is independent of the amplitude of the power spectrum and galaxy bias, b. This is because $\xi_{2,\,\mathrm{gI}}$ arises from the correlation of the galaxy density field and the selection-induced shape polarization, the latter of which is independent of bias. It does depend on the projected correlation function w_p through L. Also, since the IA signal only affects $\xi_{2,\,\mathrm{gI}}$ through $\bar{\tau}$, which can be determined in transverse bins independently, we can forecast $\xi_{2,\,\mathrm{gI}}$ beyond the projected scales used to measure $\mathcal{E}$.

[illegible] measured for this estimate are listed in Table 1

Here's a summary of all the main measurements we need to put together for our result

Tracer	z_{min}	z_{max}	N	σ^2_{E1}	ϵ_{LOS}	$\bar{\mathcal{E}}(0 < r_p < 20)$	$\bar{L}(\ldots)$	$\bar{\tau}(5 < r_p < 18)$	$\bar{\xi}_{2,\,gI}(5 < s < 80)$
LRG	0.4	0.6	529852	0.046	2.3×10^{-3}	1.8×10^{-3}	[illegible]	$5.9 \pm 0.5 \times 10^{-3}$	0.044
LRG	0.6	0.8	805[illegible]	[illegible]	[illegible]	2.1×10^{-3}	94.9 h^{-1}Mpc	$7.0 \pm 0.2 \times 10^{-2}$	0.22
LRG	0.8	1.1	896150	0.026	12.8×10^{-3}	1.8×10^{-2}	92.9 h^{-1}Mpc	$5.6 \pm 0.2 \times 10^{-2}$	0.41
ELG	0.8	1.1	591687	0.026	12.8×10^{-3}	1.9×10^{-3}	73.2 h^{-1}Mpc	$4.3 \pm 0.3 \times 10^{-2}$	0.34

Table 1. Samples and values used to estimate the RSD bias for three LRG redshift bins and the LRGxELG cross-correlation. r_p and s are given in units of h^{-1}Mpc. The tracer samples used in the top three rows were also used as the shape sample. The last row uses ELG tracers with LRG shapes. The table shows the redshift range and number N of tracers used, and properties of the shape sample: the variance of the real component of ellipticities σ^2_{E1} and the estimated selection-induced polarization of sha[illegible] have negligible statistical errors. The IA signal $\mathcal{E}(r_p)$ is measured as the ellipticity of shapes relative to the tracer sample. $L(r_p)$ is the effective LOS-distance that $\mathcal{E}(r_p)$ is averaged over. $\tau(r_p)$ is defined in Equation 9 and is a combination of $\mathcal{E}(r_p)$, $L(r_p)$, and the power spectrum. These are functions of transverse separation, r_p and are shown in this table as averages over the mark[illegible]. The final column shows the average amplitude of the anisotropic clustering created by IA; the quadrupole of the correlation function without RSD [illegible] the full estimate of this final result along with the statistical error is shown in Figure 9.

...and this is the main plot showing that result!

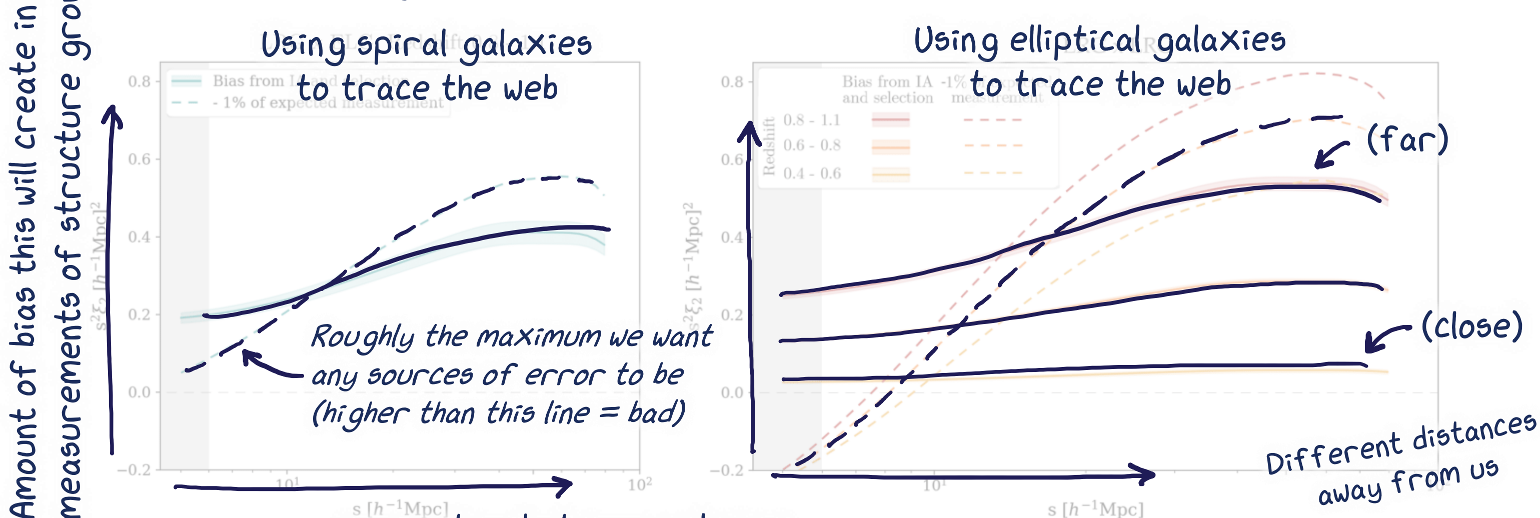

Figure 9. The anisotropic clustering signal arising from tidal alignment and a selection bias, $\xi_{2,\,gI}$. Statistical errors are shown in the shaded bands, although the total errors are dominated by systematic effects (Section 6). For context, we have also plotted 1% of the expected ξ_2 signal from RSD. This is well above DESI's error budget for measuring the growth rate of structure, which is 0.4-0.7% for LRGs and ELGs combined. Since the ξ_2 signal created by the growth of structure is opposite in sign to that created by IA, we have multiplied the RSD ξ_2 by -1 for an easier comparison. This plot demonstrates that IA will dampen DESI's [illegible] the ξ_2 measurement will mitigate this effect.

Here we repeat some information from the last paper for easy reference. The main idea is that the more galaxy correlation we see, and the more bias there is in galaxy shapes, the more DESI's measurements will be affected.

and the final quadrupole signature for all our samples is shown in Figure 9. To provide context for this signal, we estimate the total quadrupole signatures ξ_2 expected for these galaxy samples. They are based on HOD catalogs made with the ABACUSSUMMIT simulations (Hadzhiyska et al. 2021; Maksimova et al. 2021; Yuan et al. in prep. 2024), and scaled with measurements from DESI's Survey Validation (DESI Collaboration et al. 2023b). Figure 9 shows 1% of these estimates, which is well above DESI's total error budget for measuring ξ_2. Since the ξ_2 signal created by the growth of structure is opposite in sign to that created by IA, we have also multiplied this 1% line by -1 for a clear comparison. On the scales used to measure $f\sigma_8$ ($10 < s < 80\ h^{-1}$Mpc), ξ_2 for LRGs will be dampened by around 0.15% between redshifts 0.4-0.6, 0.53% between redshifts 0.6-0.8, and 0.8[illegible] cross-correlations will be biased by around 0.83% between redshifts of 0.8-1.1.

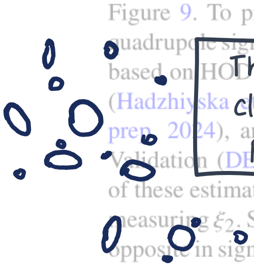

The "fake" clustering pattern ∝ How much the shapes of galaxies correlate with large-scale structure × How much galaxies in the survey tend to be pointed towards Earth

The pattern it creates is the same pattern we use to measure how structure grows.

We used a Nonlinear Alignment model, which has shown to be valid d[illegible] our estimate can be extended down to the scales of the Fingers of God effect, where peculiar velocities of galaxies create a "smearing" along th[illegible] growth (Jackson 1972). Here, the sign of ξ_2 switches and this bias will result in an enhancement of the signal. However, as nonlinear effects become more apparent here and and this effect is less relevant for DESI's main science goals, it is most valuable to interpret the [illegible] large scales.

Galaxies fall towards dense region as the web evolves. These motions affect the positions of galaxies we measure, creating a 'distortion' in the galaxy map.

6 CONCLUSION

We measure the tidal alignment of LRGs with DESI Year 1 redshifts, using both LRG and ELG tracers. We also estimate a redshift-dependent polarization in LRG orientations relative to the LOS which arises from an aperture-based target selection. Using a nonlinear tidal model, we calculate the signal this will create in DESI's measurements of the quadrupole of the correlation function. It ranges from 0.2-1.1% of the quadrupole signal created by RSD, a significant fraction of DESI's full-survey error budget of around [illegible] for measuring the growth rate with LRGs and ELGs combined. [illegible] RSD bias is over [illegible] larger in the highest redshift sample, $0.8 < z < 1.1$, than the lowest, $0.4 < z < 0.6$. This is partially due to a stronger alignment signal, but mostly due to the selection effect: galaxies at higher redshifts are redder and fainter, falling closer to the target selection cuts. Therefore their orientation has a stronger

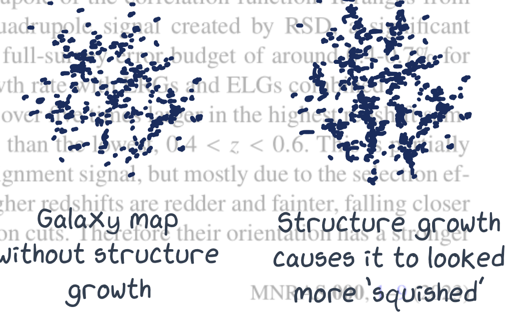

CONCLUSION

Correlations between galaxy orientations and the cosmic web combine with a bias in galaxy orientations and mess with our measurements of how the cosmic web grows.

This is not a new idea, but we are able to measure this effect with some of DESI's first data, allowing us to see how it changes with more distant galaxies. We find it's a bigger deal for more distant galaxies, mostly because they're fainter and more likely to have biased orientations.

Without the corrections in this paper, DESI could underestimate the growth rate of structure, therefore overestimating the effects of dark energy.

influence on whether or not they pass the aperture magnitude cut and the sample has a stronger orientation polarization. If uncorrected for, this redshift-dependent bias will suppress measurements of the grow[illegible] will also bias determinations of how the growth rate evolves, a critical estimator for constraining cosmological models (Kazantzidis & Periv[illegible] created by IA presented here can be used to mitigate this bias.

These results agree with the previous work in Lamman et al. (2023[illegible]) and estimated that it will produce around a 0.5% decrease on measurements of ξ_2 with the full LRG sample. While large, upcoming photometric surveys can provide constraints on IA, for this effect it's most important to understand the IA of our particular sample. Additionally, redshifts are necessary to make clean distant cuts to explore redsh[illegible].

The largest uncertainty in our final results comes from systematic effects in the estimate of the selection-induced shape polarization. This is sensitive to assumptions in the light profiles used for mock selection and the underlying triaxial distribution of shapes, which is based on SDSS imaging (Padilla & Strauss 2008) and not in clear agreement with comparable galaxies in hydrodynamic simulations (Bassett & Foster 2019). This could be significantly improved with a large imaging survey such as the Dark Energy Survey or the upcoming Legacy Survey of Space and Time (Gatti et al. 2021; Ivezić et al. 2019). The method of imaging and shape fits have a known impact on the inferred intrinsic shapes of galaxies (Georgiou et al. 2019; MacMahon & Leonard 2023).

While we do not expect a significant RSD bias from the shape alignment of ELGs, their spins are known to correlate with the tidal field (Lee [illegible]). Their shapes could also be biased in DESI's sample as spectroscopic quality depends upon disk orientation (Hirata 2009). This bias could be explored in DESI through correlations between the quadrupole of the correlation function and fundamental plane residuals (Singh et al. 2021).

The remaining four years of DESI's main survey will produce millions more spectroscopic redshifts, allowing us to refine IA measurements and their redshift dependence. These will also produce higher precision RSD measurements, necessitating the need to incorporate the anisotropic clustering effect caused by IA.

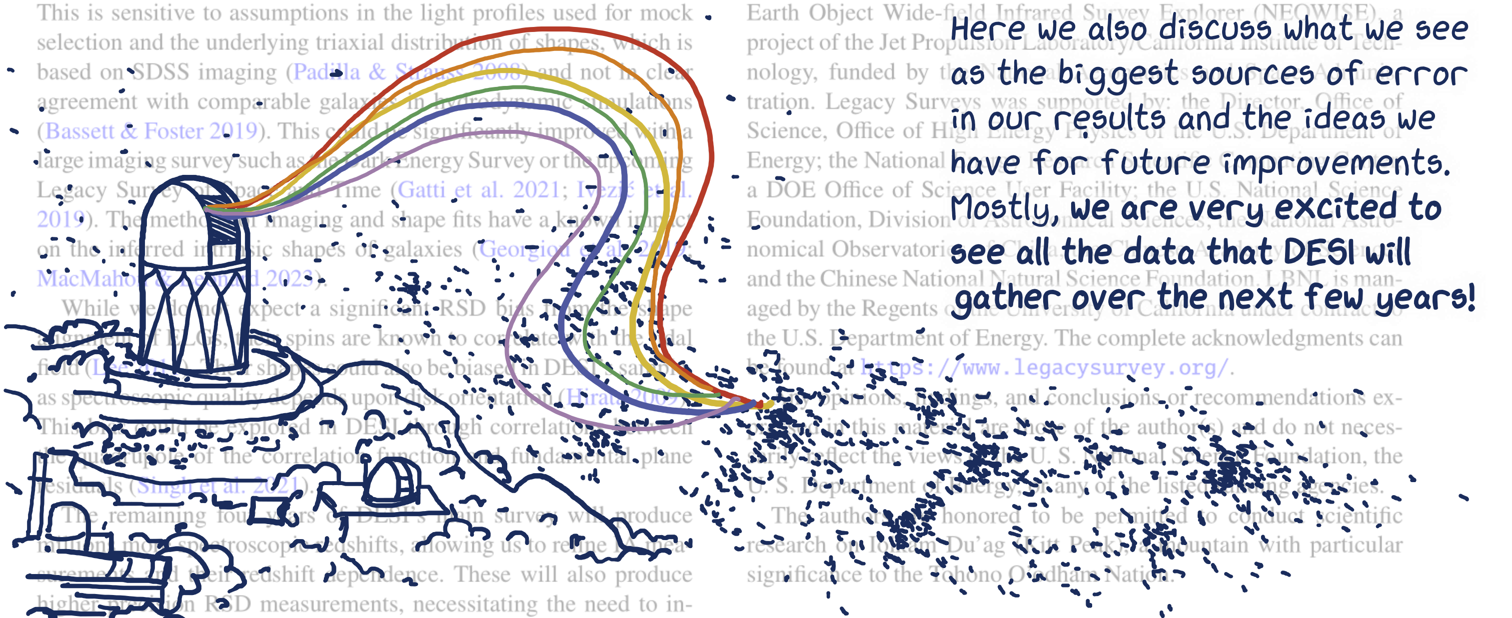

Here we also discuss what we see as the biggest sources of error in our results and the ideas we have for future improvements. Mostly, we are very excited to see all the data that DESI will gather over the next few years!

WE DIDN'T DO IT ALONE

ACKNOWLEDGEMENTS

This work received support from many places, including funding agencies and useful conversations with colleagues!

CL thanks the DESI internal reviewers of this paper, Mustapha Ishak and Benjamin Joachimi, for through feedback. CL also thanks Jonathan Blazek for several helpful discussions.

This material is based upon work supported by the National Science Foundation Graduate Research Fellowship under Grant No. DGE174[illegible] grant DE-SC0013718, NASA under ROSES grant 12-EUCLID12-0004, and the Simons Foundation.

This m[illegible] U.S. Department of Energy (DOE), Office of Science, Office of High-Energy Physics, under Contract No. DE–AC02–05CH11231, and by the National Energy Research Scientific Computing Center, a DOE Office of Science User Facility under the same contract. Additional support for DESI was provided by the U.S. National Science Foundation (NSF), Division of Astronomical Sciences under Contract No. AST-0950945 to the NSF's National Optical-Infrared Astronomy Research Laboratory; the Science and Technology Facilities Council of the United Kingdom; the Gordon and Betty Moore Foundation; the Heising-Simons Foundation; the French Alternative Energies and Atomic Energy Commission (CEA); the National Council of Science and Technology of Mexico (CONACYT); the Ministry of Science and In[illegible] and by the DESI Member Institutions: https://www.desi.lbl.gov/collaborating-institutions.

The DESI Legacy Imaging Surveys consist of three individual [illegible] vey (DECaLS), the Beijing-Arizona Sky Survey (BASS), and the Mayall z-band Legacy Survey (MzLS). DECaLS, BASS and MzLS [illegible] Cerro Tololo Inter-American Observatory, NSF's NOIRLab; the Bok telescope, Steward Observatory, University of Arizona; and the Mayall telescope, Kitt Peak National Observatory, NOIRLab. NOIRLab is operated by the Association of Universities for Research in Astronomy (AURA) under a cooperative agreement with the National Science Foundation. Pipeline processing and analyses of the data were supported by NOIRLab and the Lawrence Berkeley National Laboratory. Legacy Surveys also uses data products from the Near-Earth Object Wide-field Infrared Survey Explorer (NEOWISE), a project of the Jet Propulsion Laboratory/California Institute of Technology, funded by the National Aeronautics and Space Administration. Legacy Surveys was supported by: the Director, Office of Science, Office of High Energy Physics of the U.S. Department of Energy; the National Energy Research Scientific Computing Center, a DOE Office of Science User Facility; the U.S. National Science Foundation, Division of Astronomical Sciences; the National Astronomical Observatories of China, the Chinese Academy of Sciences and the Chinese National Natural Science Foundation. LBNL is managed by the Regents of the University of California under contract to the U.S. Department of Energy. The complete acknowledgments can be found at https://www.legacysurvey.org/.

Any opinions, findings, and conclusions or recommendations expressed in this material are those of the author(s) and do not necessarily reflect the views of the U. S. National Science Foundation, the U. S. Department of Energy, or any of the listed funding agencies.

The authors are honored to be permitted to conduct scientific research on Iolkam Du'ag (Kitt Peak), a mountain with particular significance to the Tohono O'odham Nation.

SEE THE DATA YOURSELF

DATA AVAILABILITY

You can find the publicly available data we used here

The DESI Legacy Imaging Survey is publicly available at legacysurvey.org and DESI's Early Data Release is publicly available at data.desi.lbl.gov/[illegible] DESI Year 1 sample and will be publicly released as part of DESI Data Release 1 (DR1). AbacusSu[illegible] abacusnbody.org. Code for projecting ellipsoids and generating light profiles can be found at github.com/cmlamman/ellipse_alignment.

Data plotted in this paper are available at zenodo.org/uploads/10162040.

WE DIDN'T START FROM SCRATCH

REFERENCES

This project is built upon the work and ideas of others, and is part of an ongoing scientific conversation

Bassett R., Foster C., 2019, Monthly Notices of the Royal Astronomical Society, 487, 2354

Chisari N. E., [illegible] Physics, 12, 020

DESI Collaboration et al., 2016a, Technical report, The DESI Experiment [illegible] https://ui.adsabs.harvard.edu/abs/2016arXiv161100036D,

doi:10.48550/arXiv.1611.00036, https://ui.adsabs.harvard.edu/abs/2016arXiv161100036D
DESI Collaboration et al., 2016b, Technical report, The DESI Experiment Part II: Instrument Design, https://ui.adsabs.harvard.edu/abs/2016arXiv161100037D. Lawrence Berkeley National Laboratory, https://ui.adsabs.harvard.edu/abs/2016arXiv161100037D
DESI Collaboration et al., 2022, The Astronomical Journal, 164, 207
DESI Collaboration et al., 2023a, The Early Data Release of the Dark Energy Spectroscopic Instrument, doi:10.48550/arXiv.2306.06308, https://ui.adsabs.harvard.edu/abs/2023arXiv230606308D
DESI Collaboration et al., 2023b, Validation of the Scientific Program for the Dark Energy Spectroscopic Instrument, doi:10.48550/arXiv.2306.06307, https://ui.adsabs.harvard.edu/abs/2023arXiv230606307D
Dey A., et al., 2019, The Astronomical Journal, 157, 168
Fasano G., Bonoli C., 1989, Astronomy and Astrophysics Supplement Series, 79, 291
Gatti M., et al., 2021, Monthly Notices of the Royal Astronomical Society, 504, 4312
Georgiou C., et al., 2019, Astronomy and Astrophysics, 622, A90
Guy J., et al., 2023, The Astronomical Journal, 165, 144
Hadzhiyska B., Eisenstein D., Bose S., Garrison L. H., Maksimova N., 2021, Monthly Notices of the Royal Astronomical Society, 509, 501
Hirata C. M., 2009, Monthly Notices of the Royal Astronomical Societ… 99, 1074
Ivezić , et al., 2019, The Astrophysical Journal, 873, 111
Jackson J. C., 1972, Monthly Notices of the Royal Astronomical S… 1P
Joachimi B., et al., 2015, Space Science Reviews, 193, 1
Johnston H., et al., 2019, Astronomy and Astrophysics, 624, A30
Kaiser N., 1987, Monthly Notices of the Royal Astronomical Soci…
Kazantzidis L., Perivolaropoulos L., 2021, 8 Tension. Is Gravity … Weaker at Low z? Observational Evidence and Theoretical Impl… cations, doi:10.1007/978-3-030-83715-0_33, https://ui.adsabs.harvard.edu/abs/2021mgca.book..507K
Kurita T., Takada M., 2023, Constraints on anisotropic primordial non-Gaussianity from intrinsic alignments of SDSS-III BOSS galaxies, doi:10.48550/arXiv.2302.02925, https://ui.adsabs.harvard.edu/abs/2023arXiv230202925K
Lamman C., Tsaprazi E., Shi J., Niko Šarčević N., Pyne S., Legnani E., Ferreira T., 2023a, The IA Guide: A Breakdown of Intrinsic Alignment Formalisms, doi:10.48550/arXiv.2309.08605, https://ui.adsabs.harvard.edu/abs/2023arXiv230908605L
Lamman C., et al., 2023b, Monthly Notices of the Royal Astronomical Society, 522, 117
Lan T.-W., et al., 2023, The Astrophysical Journal, 943, 68
Lang D., Hogg D. W., Mykytyn D., 2016, Astrophysics Source Code Library, p. ascl:1604.008
Lee J., 2011, The Astrophysical Journal, 732, 99
Leonard C. D., Mandelbaum R., Collaboration L. D. E. S., 2018, Monthly Notices of the Royal Astronomical Society, 479, 1412
Levi M., et al., 2013, The DESI Experiment, a whitepaper for Snowmass 2013, doi:10.48550/arXiv.1308.0847, https://ui.adsabs.harvard.edu/abs/2013arXiv1308.0847L
MacMahon C. M. B., Leonard C. D., 2023
Maksimova N. A., Garrison L. H., Eisenstein D. J., Hadzhiyska B., Bose S., Satterthwaite T. P., 2021, Monthly Notices of the Royal Astronomical Society, 508, 4017
Mandelbaum R., Hirata C. M., Ishak M., Seljak U., Brinkmann J., 2006, Monthly Notices of the Royal Astronomical Society, 367, 611
Martens D., Hirata C. M., Ross A. J., Fang X., 2018, Monthly Notices of the Royal Astronomical Society, 478, 711
Myers A. D., et al., 2023, The Astronomical Journal, 165, 50
Obuljen A., Percival W. J., Dalal N., 2020, Journal of Cosmology and Astroparticle Physics, 2020, 058
Okumura T., Taruya A., 2023, The Astrophysical Journal, 945, L30
Padilla N. D., Strauss M. A., 2008, Monthly Notices of the Royal Astronomical Society, 388, 1321
Raichoor A., et al., 2020, Research Notes of the American Astronomical Society, 4, 180
Raichoor A., et al., 2023, The Astronomical Journal, 165, 126
Samuroff S., et al., 2019, Monthly Notices of the Royal Astronomical Society, 489, 5453
Samuroff S., Mandelbaum R., Blazek J., 2021, Monthly Notices of the Royal Astronomical Society, 508, 637
Samuroff S., et al., 2023, Monthly Notices of the Royal Astronomical Society, 524, 2195
Singh S., Mandelbaum R., More S., 2015, Monthly Notices of the Royal Astronomical Society, 450, 2195
Singh S., Yu B., Seljak U., 2021, Monthly Notices of the Royal Astronomical Society, 501, 4167
Troxel M. A., Ishak M., 2015, Physics Reports, 558, 1
Xu K., Jing Y. P., Zhao G.-B., Cuesta A. J., 2023, Nature Astronomy, 7, 1259
Yuan et al. in prep. S., 2024
Zhou R., et al., 2020, Research Notes of the American Astronomical Society, 4, 181
Zhou R., et al., 2022, Technical report, Target Selection and Validation of DESI Luminous Red Galaxies, https://ui.adsabs.harvard.edu/abs/2022arXiv220808515Z. https://ui.adsabs.harvard.edu/abs/2022arXiv220808515Z
Zh… al., 2023, Monthly Notices of the Royal Astronomical Society, …323
…2017, Publications of the Astronomical Society of the Pacific, …101
… al., 2018, Monthly Notices of the Royal Astronomical Society, …1149

…er has been typeset from a TEX/LATEX file prepared by the author.

To learn more about DESI, check out desi.lbl.gov

For a similar paper summary on Dark Energy, see this link
For a similar paper summary on a related paper, see this link.

If you've gotten this far, CONGRATULATIONS!
I hope my notes made it easier to digest this paper. If you're a scientist, I would love to read similar notes on one of your papers :)
– Claire Lamman

I made this in power point using the XKCD font:
https://github.com/ipython/xkcd-font